The Astrophysical Journal, 624:28–33, 2005 May 1

VELOCITY EFFECTS ON THE DEFLECTION OF LIGHT BY GRAVITATIONAL MICROLENSES

David Heyrovský
Institute of Theoretical Physics, Charles University, V Holešovičkách 2, 180 00 Prague, Czech Republic; david.heyrovsky@mff.cuni.cz
Received 2004 September 28; accepted 2005 January 18

ABSTRACT

We study the influence of general lens and source velocities on the gravitational deflection of light by single and two–point-mass microlenses with general axis orientation. We compute the deflection angle and demonstrate that in all cases the lens equation preserves its form exactly. However, the Einstein radius and the separation of the two lenses depend on the lens velocity. In Galactic microlensing settings the velocity mainly affects the inferred separation for tangentially moving wide binary star or star+planet microlenses oriented close to the line of sight. We briefly discuss the case of lenses moving with highly relativistic velocities.

Subject headings: gravitational lensing — relativity

1. INTRODUCTION

The time dependence of Galactic gravitational microlensing events (Paczyński 1996) is given by the relative motion of the source of light, the lens, and the observer near perfect alignment. These events have been generally successfully analyzed using a quasistatic approach, assuming that the observed light has been deflected in a static source-lens-observer configuration at each instant. This approach is well justified because the lens and source velocities relative to the observer are on the order of a couple hundred km s^{-1}, i.e., $\sim 10^{-3}$ of the speed of light c.

Nevertheless, with the introduction of image subtraction techniques (Alard & Lupton 1998) the accuracy of measured microlensing light curves has increased in ideal cases to subpercent levels. In addition, there are prospects for high-precision observations of the astrometric microlensing effect (see Boden et al. [1998] and Han [2001] for the single and binary lens cases, respectively) by space-based interferometers such as the *Space Interferometry Mission*.[1] Given these developments, one can expect that corrections to the light curve or the angular image geometry down to the order of $\sim 10^{-3}$ may be detectable. It is therefore interesting to avoid the quasistatic approach and investigate the effect of general lens and source velocities on light deflection and the inferred lensing parameters.

Previous theoretical research has mostly concentrated on the effect of a relative lens-to-observer velocity on the deflection angle by a single lens. Pyne & Birkinshaw (1993) derived the effect to first order in v/c for a velocity of arbitrary direction, showing that the deflection angle increased for lenses moving away from the observer and decreased for those moving toward the observer. The same result was later confirmed by Frittelli (2003). Recently Wucknitz & Sperhake (2004) presented results for an arbitrarily large but purely radial lens velocity. The most general theoretical result can be found in the detailed treatise by Kopeikin & Schäfer (1999), which includes a derivation of the deflection angle for an ensemble of lenses of general velocities.

In this paper we study light deflection for general lens and source velocities (arbitrarily oriented and arbitrarily large), specifically for single and two–point-mass lens microlensing events. In § 2 we derive the general lens equation and demonstrate the velocity dependence of its parameters. In § 3 we explore the magnitude of the velocity effects for low velocities and illustrate the highly relativistic limit. We conclude in § 4 by discussing observational aspects and the appropriateness of some of the assumptions, and we summarize the main results in § 5.

[1] See http://sim.jpl.nasa.gov.

2. DERIVATION OF LENS EQUATION

Our approach is similar to the one used by Klioner (2003) for a single lens in motion. We use the knowledge of light-deflection formulae in the rest frame of the lens and, using Lorentz transformations, connect the solution to the rest frame of the observer. We limit our accuracy to the usual first order in deflection angle. This means that, for example, light rays passing close to the components of a binary pulsar are thus beyond the scope of this paper.

In the case of two–point-mass lenses (includes binary star and star+planet lens systems, hereafter "binary lenses" for brevity) we concentrate on the effect of their center-of-mass velocity and neglect the effect of orbital velocity. This approach is justifiable for sufficiently wide binaries (with semimajor axis $\gtrsim 1$ AU). We return to the case of closer binaries in § 4.

For the purposes of the following calculation we set up the observer rest-frame coordinates with the origin at the center of mass of the lens at observer time $t' = 0$, the z'-axis pointing toward the observer, the x'-axis in the plane of the sky along the projected binary lens axis, and the y'-axis perpendicular to it in the plane of the sky. We denote the distance between the observer and the (center of mass of the) lens D_L, the distance between the observer and the source plane D_S, and the distance between the lens and source planes D_{LS}.

For simplicity we scale all velocities to the speed of light. We denote the lens and source velocities measured in the rest frame of the observer $\boldsymbol{V}$ and $\boldsymbol{W}$, respectively. At time t' in the described observer rest frame, the observer, the center of mass of the lens, and the source are located at

$$\begin{aligned} \boldsymbol{r}'_O &= (0,\, 0,\, D_L), \\ \boldsymbol{r}'_L(t') &= \boldsymbol{V}t', \\ \boldsymbol{r}'_S(t') &= \boldsymbol{r}'_{S0} + \boldsymbol{W}(t' + D_{LS}), \end{aligned} \tag{1}$$

respectively. In the last expression $\boldsymbol{r}'_{S0} = (\beta_1 D_S,\, \beta_2 D_S,\, -D_{LS})$ is the source position at $t' = -D_{LS}$. The two-dimensional angle $\boldsymbol{\beta}$ is the angular position of the source in the plane of the sky. Note that an undeflected photon arriving at the observer at

$t' = D_L$ passed the lens at $t' = 0$ and the source at $t' = -D_{LS}$. The lens and source velocities and distances are thus measured at these retarded times.

We denote the total mass of the lens M; in the binary lens case the two lensing bodies have masses $M_A \equiv \mu_A M$ and $M_B \equiv \mu_B M$, respectively. As hinted earlier, we place no restrictions on the mass ratio of the two lenses; our results thus hold for single and binary star lenses, as well as for star+planet lenses. We define the coordinates in the rest frame of the lens with their origin at the center of mass of the lens, the x-axis along the physical binary lens axis, the y-axis in the plane of the sky parallel to y', and the z-axis perpendicular to both. In these coordinates the lenses are located at $\boldsymbol{r}_A = (-\mu_B R,\ 0,\ 0)$ and $\boldsymbol{r}_B = (\mu_A R,\ 0,\ 0)$, where R is the distance between them (their intrinsic separation). We denote the angle between the binary lens axis and the plane of the sky ζ, oriented so that a small positive ζ brings lens A closer to the observer. The directions of the x- and z-axes thus coincide with those of the observer's x' and z' only if the binary lens axis lies in the plane of the sky, i.e., $\zeta = 0^\circ$.

We denote the future asymptotic trajectory of a photon (at the observer) in lens-frame coordinates

$$\boldsymbol{r}_{po}(t) = \boldsymbol{l} + \boldsymbol{n}_0 t, \tag{2}$$

where $\boldsymbol{n}_0$ is a unit vector and the past asymptotic trajectory of the photon (at the source) is

$$\boldsymbol{r}_{ps}(t) = \boldsymbol{r}_{po}(t) + \frac{4G}{c^2} \times \sum_{i=A,\,B} M_i \frac{\boldsymbol{n}_0 \cdot [\boldsymbol{r}_{po}(t) - \boldsymbol{r}_i]}{[\boldsymbol{n}_0 \times (\boldsymbol{l} - \boldsymbol{r}_i)]^2} [\boldsymbol{l} - \boldsymbol{r}_i - \boldsymbol{n}_0 \cdot (\boldsymbol{l} - \boldsymbol{r}_i)\, \boldsymbol{n}_0], \tag{3}$$

as demonstrated, for example, in Will (1981) or Brumberg (1991). To obtain the values of the constant vectors $\boldsymbol{l}$ and $\boldsymbol{n}_0$ in terms of physical parameters, we transform the future asymptotic trajectory to observer-frame coordinates, in which the trajectory of a photon arriving at the observer is

$$\boldsymbol{r}'_{po}(t') = \boldsymbol{r}'_O + \boldsymbol{n}'_0 (t' - D_L). \tag{4}$$

The unit vector $\boldsymbol{n}'_0 = (1 + \theta^2)^{-1/2}\,(-\theta_1,\ -\theta_2,\ 1)$ describes the direction of photon propagation at arrival. The two-dimensional angle $\boldsymbol{\theta}$ denotes the angular displacement of the image of the lensed source in the plane of the sky from the center of mass of the lens (as it would be observed at the same time).

The conversion between the two coordinate systems is given by

$$\begin{pmatrix} t' \\ \boldsymbol{r}'_{po}(t') \end{pmatrix} = \Lambda(\boldsymbol{V}) \begin{pmatrix} t \\ \mathbf{T}(\zeta)\boldsymbol{r}_{po}(t) \end{pmatrix}, \tag{5}$$

where the rotation matrix

$$\mathbf{T}(\zeta) = \begin{pmatrix} \cos\zeta & 0 & \sin\zeta \\ 0 & 1 & 0 \\ -\sin\zeta & 0 & \cos\zeta \end{pmatrix} \tag{6}$$

corrects for the orientation of the binary lens axis and the components of the Lorentz boost matrix Λ (e.g., Misner et al. 1973) are

$$\Lambda^{0'}{}_0 = \gamma, \quad \Lambda^{0'}{}_i = \Lambda^{i'}{}_0 = \gamma V_i, \quad \Lambda^{i'}{}_j = \delta^{ij} + \frac{V_i V_j}{V^2}(\gamma - 1), \tag{7}$$

with $\gamma = (1 - V^2)^{-1/2}$. We express $\boldsymbol{r}_{po}(t)$ from equation (5), and by comparison with equation (2) we get the two vectors $\boldsymbol{l}$ and $\boldsymbol{n}_0$ describing the future asymptotic light ray in the lens frame:

$$\boldsymbol{l} = \mathbf{T}(-\zeta)\left\{\boldsymbol{r}'_O + \frac{D_L}{1 - \boldsymbol{V}\cdot\boldsymbol{n}'_0} \times \left[\frac{1 - \sqrt{1 - V^2}}{V^2}(\boldsymbol{V}\cdot\boldsymbol{n}'_0 - V_z)\boldsymbol{V} - (1 - V_z)\boldsymbol{n}'_0\right]\right\},$$

$$\boldsymbol{n}_0 = \frac{1}{1 - \boldsymbol{V}\cdot\boldsymbol{n}'_0}\mathbf{T}(-\zeta) \times \left[\left(\frac{1 - \sqrt{1 - V^2}}{V^2}\boldsymbol{V}\cdot\boldsymbol{n}'_0 - 1\right)\boldsymbol{V} + \sqrt{1 - V^2}\boldsymbol{n}'_0\right]. \tag{8}$$

In a similar way we can take the expression for the past asymptotic trajectory of the photon from equation (3) and extend it to the source as follows:

$$\begin{pmatrix} t'_e \\ \boldsymbol{r}'_S(t'_e) \end{pmatrix} = \Lambda(\boldsymbol{V}) \begin{pmatrix} t_e \\ \mathbf{T}(\zeta)\boldsymbol{r}_{ps}(t_e) \end{pmatrix}. \tag{9}$$

Note that $\boldsymbol{r}'_S(t'_e)$ depends on the source velocity $\boldsymbol{W}$; see equation (1). To get the photon position $\boldsymbol{r}_{ps}(t_e)$, we substitute the light-ray vectors $\boldsymbol{l}$ and $\boldsymbol{n}_0$ from equation (8) into equation (3). We first use the time component of equation (9) to convert between the emission times t_e and t'_e in the two coordinate systems:

$$t'_e = (1 - \boldsymbol{V}\cdot\boldsymbol{W})^{-1}(\sqrt{1 - V^2}\,t_e + \boldsymbol{V}\cdot\boldsymbol{r}'_{S0} + \boldsymbol{V}\cdot\boldsymbol{W}D_{LS}). \tag{10}$$

We then use the z-component to eliminate the emission time altogether. From the remaining two equations we can finally express the light-deflection angle $\boldsymbol{\alpha} \equiv (\boldsymbol{\theta} - \boldsymbol{\beta})D_S/D_{LS}$ measured by the observer. Although this part of the calculation is fairly tedious, it is entirely straightforward. In the single lens case we get to first order in deflection angle

$$\boldsymbol{\alpha}(\boldsymbol{\theta}) = \frac{4GM(1 - V_z)}{c^2 D_L \sqrt{1 - V^2}}\frac{\boldsymbol{\theta}}{\theta^2}. \tag{11}$$

This expression is in agreement with the previous results of Kopeikin & Schäfer (1999) and extends the results of Pyne & Birkinshaw (1993), Frittelli (2003), and Wucknitz & Sperhake (2004). In the binary lens case we get to first order in deflection angle

$$\boldsymbol{\alpha}(\boldsymbol{\theta}) = \frac{4GM(1 - V_z)}{c^2 D_L \sqrt{1 - V^2}}\left(\mu_A \frac{\boldsymbol{\theta} - \boldsymbol{\theta}_A}{|\boldsymbol{\theta} - \boldsymbol{\theta}_A|^2} + \mu_B \frac{\boldsymbol{\theta} - \boldsymbol{\theta}_B}{|\boldsymbol{\theta} - \boldsymbol{\theta}_B|^2}\right), \tag{12}$$

where $\boldsymbol{\theta}_A \equiv -\mu_B \boldsymbol{\theta}_{AB}$ and $\boldsymbol{\theta}_B \equiv \mu_A \boldsymbol{\theta}_{AB}$ are the apparent angular positions of the two lenses and the apparent angular separation vector (from lens A to lens B) in the plane of the sky is

$$\boldsymbol{\theta}_{AB}(\boldsymbol{V}) = \frac{1}{D_L}\left[\boldsymbol{R}_\perp + \left(R_z - \frac{1 - \sqrt{1 - V^2}}{V^2}\boldsymbol{V}\cdot\boldsymbol{R}\right)\frac{\boldsymbol{V}_\perp}{1 - V_z}\right]. \tag{13}$$

Here the tangential lens velocity $\boldsymbol{V}_\perp \equiv (V_x,\ V_y)$, and the vector $\boldsymbol{R} \equiv (\boldsymbol{R}_\perp,\ R_z) = \mathbf{T}(\zeta)(\boldsymbol{r}_B - \boldsymbol{r}_A)$ is the separation vector of the two lenses at time $t' = 0$ in their center-of-mass rest frame rotated to

coincide with the orientation of the observer's axes. Its component $\boldsymbol{R}_\perp$ lies in the plane of the sky, and R_z is oriented along the line of sight to the observer (for a positive R_z, lens B lies closer to the observer).

The first obvious result is the independence of the deflection angle on the source velocity $\boldsymbol{W}$, even though the aberration between the source and the lens obviously depends on it. We note that we have demonstrated this only to first order in deflection angle and that the source velocity might have an influence at a higher accuracy. Another interesting property to note is that the *single-lens* deflection angle does not have a component in the direction of the (projected) lens velocity. Clearly, the aberration effect on the orientation of the deflection angle drops out in this first-order computation because of the two Lorentz transformations.

The dominant effect on the apparent angular separation in equation (13) is due to the photon travel time between the two lenses. To first order in lens velocity, the distance (and thus also the light-travel time) between the two lens planes is R_z. As seen by the observer, during this time the lenses move by $R_z\boldsymbol{V}_\perp$ in the plane of the sky. The effect may decrease or increase the apparent angular separation, *as well as change its orientation*, depending on the mutual orientation of the binary axis and the lens velocity (see § 3 for a more detailed discussion). The full expression in equation (13) can also be derived similarly by computing the lens positions in the observer's rest frame and taking into account their shift during the time it takes light to travel between the two lens planes.

The structure of equations (11) and (12) allows us to readily define the velocity-dependent angular Einstein radius

$$\theta_{\rm E}(\boldsymbol{V}) \equiv \sqrt{\frac{4GMD_{LS}}{c^2 D_L D_S}\frac{1-V_z}{\sqrt{1-V^2}}}. \tag{14}$$

We can rescale all angular quantities by $\theta_{\rm E}(\boldsymbol{V})$ and thus convert from $\{\boldsymbol{\beta}, \boldsymbol{\theta}, \boldsymbol{\theta}_A, \boldsymbol{\theta}_B, \boldsymbol{\theta}_{AB}\}$ to $\{\boldsymbol{y}, \boldsymbol{x}, \boldsymbol{x}_A, \boldsymbol{x}_B, \boldsymbol{d}\}$ in the usual lensing notation. The lens equation obtained for a single lens is

$$\boldsymbol{y} - \boldsymbol{x} = -\frac{\boldsymbol{x}}{x^2}, \tag{15}$$

and for a binary lens

$$\boldsymbol{y} - \boldsymbol{x} = -\mu_A \frac{\boldsymbol{x} - \boldsymbol{x}_A}{|\boldsymbol{x} - \boldsymbol{x}_A|^2} - \mu_B \frac{\boldsymbol{x} - \boldsymbol{x}_B}{|\boldsymbol{x} - \boldsymbol{x}_B|^2}. \tag{16}$$

This interesting result shows that in either case the lens equation has exactly the same form as in the static approximation. When analyzing microlensing observations, one can thus use exactly the same formulae as in the usual quasistatic approach. However, when interpreting the fitted parameters one has to realize that the Einstein radius, and in the binary lens case also the lens positions and their separation, depends on the lens velocity. Instead of $\theta_{\rm E}(0)$, one obtains $\theta_{\rm E}(\boldsymbol{V})$, and instead of the Einstein radius–scaled projected lens-separation vector $\boldsymbol{d}(0) \equiv \boldsymbol{R}_\perp/[D_L\theta_{\rm E}(0)]$, one obtains

$$\boldsymbol{d}(\boldsymbol{V}) = \frac{(1-V^2)^{1/4}}{\sqrt{1-V_z}}\left(\boldsymbol{d}(0) + \left\{d_z - \frac{1-\sqrt{1-V^2}}{V^2} \times \left[V_z d_z + \boldsymbol{V}_\perp \cdot \boldsymbol{d}(0)\right]\right\}\frac{\boldsymbol{V}_\perp}{1-V_z}\right), \tag{17}$$

where $d_z \equiv R_z/[D_L\theta_{\rm E}(0)]$ is the z-component of the binary lens separation vector (the "depth" of the binary lens along the line of sight) rescaled by the static Einstein radius of the lens.

The velocity dependence thus introduces a further degeneracy of the parameters of the lens equations. A difference in velocities can cause different lens systems (e.g., differently oriented binaries) to produce similar microlensing effects. In the following section we study the velocity effect on the lensing parameters in order to assess its potential influence on the inferred physical parameters of the microlenses.

3. VELOCITY EFFECTS ON INFERRED LENSING PARAMETERS

Light-curve analysis of simple microlensing events does not directly yield the angular scale of the event geometry. Event parameters such as the Einstein radius crossing time and the impact parameter are obtained scaled to $\theta_{\rm E}$ and thus will be affected in the same way as the Einstein radius. In addition, the scaled lens separation in the binary lens case will be affected as shown by equation (17).

In events beyond the simple model, such as caustic-crossing (source-transit) events or parallax events, as well as in events observed astrometrically, it is also possible to measure the angular scale. Therefore, in such events the effect on the angular Einstein radius and the angular lens separation given by expression (13) is potentially of interest.

In the following subsections we study the effects of the lens velocity on the angular Einstein radius $\theta_{\rm E}(\boldsymbol{V})$, the angular lens separation $\boldsymbol{\theta}_{AB}(\boldsymbol{V})$, and the Einstein radius–scaled lens separation $\boldsymbol{d}(\boldsymbol{V})$. In § 3.1 we explore the low-velocity case, which is astrophysically relevant for typical Galactic microlensing settings. In § 3.2 we discuss the high-velocity results.

3.1. *Low Velocities*

The second-order $V \ll 1$ expansions of expressions (14), (13), and (17) are

$$\begin{aligned}
\theta_{\rm E}(\boldsymbol{V}) &\simeq \theta_{\rm E}(0)\left(1 - \frac{V_z}{2} + \frac{2V_\perp^2 + V_z^2}{8}\right),\\
\boldsymbol{\theta}_{AB}(\boldsymbol{V}) &\simeq \boldsymbol{\theta}_{AB}(0)\\
&\quad + \frac{1}{D_L}\left[R_z\boldsymbol{V}_\perp + \frac{1}{2}(V_z R_z - \boldsymbol{V}_\perp\cdot\boldsymbol{R}_\perp)\boldsymbol{V}_\perp\right],\\
\boldsymbol{d}(\boldsymbol{V}) &\simeq \boldsymbol{d}(0)\left(1 + \frac{V_z}{2} + \frac{V_z^2 - 2V_\perp^2}{8}\right)\\
&\quad + \boldsymbol{V}_\perp\left[(1+V_z)d_z - \frac{1}{2}\boldsymbol{V}_\perp\cdot\boldsymbol{d}(0)\right],
\end{aligned} \tag{18}$$

where $\boldsymbol{\theta}_{AB}(0) = \boldsymbol{R}_\perp/D_L$. The angular Einstein radius has a linear-order effect only if the lens has a nonzero radial velocity, whereas any purely tangential velocity produces a nonzero second-order effect. As expected from previous results, the radius increases for lenses moving away from the observer and decreases for those moving toward the observer. However, even a 10^{-3} effect on $\theta_{\rm E}$ requires an unlikely radial velocity $cV_z \simeq 600$ km s^{-1}. We conclude that the effect of lens velocity on the angular Einstein radius is currently not observationally significant in Galactic microlensing.

From equation (13) we can see that any purely radial velocity of the lens has no effect on the apparent *angular* separation of the lenses $\boldsymbol{\theta}_{AB}$. The angular separation vector has a linear-order effect only if the binary lens has a nonzero tangential velocity

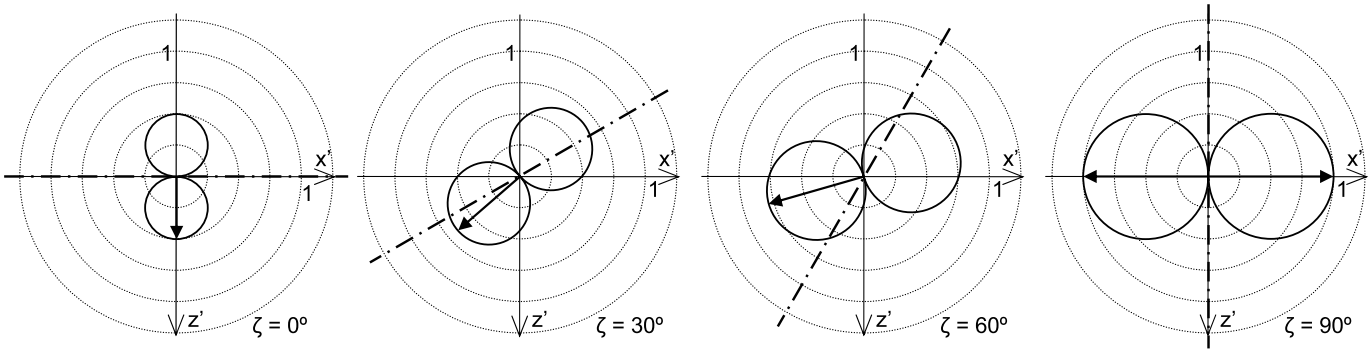

FIG. 1.—Radially plotted effect of velocity on binary lens separation $d(\boldsymbol{V}) - d(0)$ given by eqs. (19)–(20), depending on velocity direction in the observer+binary plane (z'-axis points to observer; x'-axis in the plane of the sky). Individual plots are for different binary axis orientations ζ (*dot-dashed lines: binary axis*). The effect is radially scaled in units of $V[d^2(0) + d_z^2]^{1/2}$, and the circles are spaced by 0.25. Arrows mark the direction of maximum positive effect given by eq. (21). Three-dimensional extensions of the plots are rotationally symmetric: for $\zeta \neq 90^\circ$, around the arrow; for $\zeta = 90^\circ$, around the z'-axis.

and at the same time its axis is tilted from the plane of the sky, as shown in the previous section. The effect is oriented along the vector of the tangential velocity, and its direction depends on the sign of R_z. The magnitude of the relative effect $[\theta_{AB}(\boldsymbol{V})/\theta_{AB}(0) - 1]$ is $R_z(\boldsymbol{V}_\perp \cdot \boldsymbol{R}_\perp)/R_\perp^2$, with a maximum value of $V_\perp \tan\zeta$ for a purely tangential velocity parallel to the projected binary lens axis. A low value of $V_\perp$ can thus be offset by a high angle of inclination of the binary lens axis. For a tangential velocity $cV_\perp = 200$ km s^{-1} we get a 1% effect for $\zeta = 86^\circ$, which corresponds for example to a projected separation $R_\perp \approx 1$ AU for a binary lens with a physical separation $R \approx 15$ AU. The geometric conditions required for even higher effects are no less realistic. We see that the effect is observationally significant for binary star or star+planet lenses aligned nearly along the line of sight.

To investigate the effect of velocity on the size of the Einstein radius–scaled lens-separation vector $d(\boldsymbol{V})$, we have to treat separately binary lenses oriented along the line of sight, for which $d(0) = 0$. In this case the first-order absolute effect is

$$d(\boldsymbol{V}) - d(0) \simeq |d_z \boldsymbol{V}_\perp|. \tag{19}$$

For a given total velocity V the maximum effect $V|d_z|$ occurs for a purely tangential velocity. The zero minimum effect occurs for a purely radial lens velocity.

For a general binary lens not oriented along the line of sight, $d(0) > 0$, and the first-order absolute effect is

$$d(\boldsymbol{V}) - d(0) \simeq \frac{V_z}{2} d(0) + \frac{\boldsymbol{V}_\perp \cdot \boldsymbol{d}(0)}{d(0)} d_z. \tag{20}$$

A straightforward computation shows that the maximum value of $V[d^2(0) + 4d_z^2]^{1/2}/2$ is achieved for a velocity orientation

$$\boldsymbol{V} = \frac{V}{R_z\sqrt{1 + 4R_z^2/R_\perp^2}} \left[\left(2\frac{R_z^2}{R_\perp^2} - 1 \right) \boldsymbol{R}_\perp + \boldsymbol{R} \right]. \tag{21}$$

The minimum value has the same effect with a negative sign and occurs for an opposite velocity, whereas a zero effect occurs for velocities perpendicular to velocity (21). It is interesting to note that for a given binary axis orientation the maximum effect on the scaled lens separation occurs generally for a different velocity orientation than the maximum effect on the angular lens separation.

Figure 1 illustrates the dependence of the absolute first-order effect on the direction of the lens velocity for different orientations of the binary lens axis. As seen in the fourth image and discussed above, the overall maximum effect occurs for radially oriented binary lenses ($\zeta = 90^\circ$) moving tangentially, i.e., in the plane of the sky. The maximum effect for tangentially oriented binary lenses ($\zeta = 0^\circ$; Fig. 1, *first image*) is half as large and occurs in the case of radial motion. For both these extreme binary orientations, motion in the direction of their axis causes a zero first-order effect. In terms of lensing parameters, the maximum first-order absolute effect for a binary lens with its axis tilted by ζ from the plane of the sky is

$$d(\boldsymbol{V}) - d(0) \simeq 0.01 \frac{\sqrt{1 + 3\sin^2\zeta}}{2} \frac{cV}{200 \text{ km s}^{-1}} \times \left[\frac{\theta_E(0)}{1 \text{ mas}} \right]^{-1} \frac{R}{60 \text{ AU}} \left(\frac{D_L}{4 \text{ kpc}} \right)^{-1} \tag{22}$$

for a velocity direction given by equation (21). The effect for higher lens velocities, wider intrinsic lens separations R, and lower Einstein radii can thus be a significant fraction of the Einstein radius. The maximum relative effect $[d(\boldsymbol{V})/d(0) - 1]$ is $V(\cos^{-2}\zeta - 0.75)^{1/2}$, which is largest for $\zeta \to 90^\circ$. In this regime it coincides with the maximum relative effect for the angular separation θ_{AB} derived above.

To summarize the low-velocity results, first-order effects are caused by the radial velocity of the lens and/or the "depth" of the binary lens along the line of sight. In the case of a single lens, the effect of lens velocity on the inferred lensing parameters is not significant. In the case of binary star or star+planet lenses, the inferred values of the angular and Einstein radius–scaled lens separations (as well as the linearly related lens positions) can differ from the values at zero velocity by more than 1%, mostly for tangentially moving lens systems with their axes oriented close to the line of sight. In particular, the effect on the scaled lens separation can be a significant fraction of the Einstein radius mainly for lenses with wide intrinsic separations.

3.2. *High Velocities*

The general dependence of the angular Einstein radius on the lens velocity as given by equation (14) is illustrated in Figure 2. We can see that the high-velocity effects depend on the direction of the velocity. In particular, the case when the lens moves directly toward the observer has to be treated separately.

If we increase the velocity $V \to 1$ in any other direction (including directly away from the observer), the angular Einstein radius eventually diverges, $\theta_E(\boldsymbol{V}) \to \infty$. Equation (13) gives us

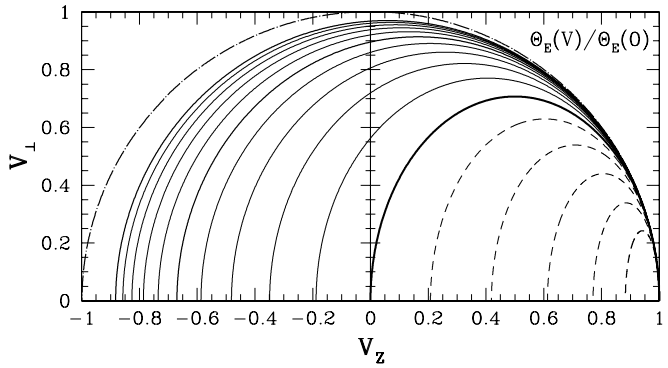

FIG. 2.—Contour plot of Einstein radius ratio $\theta_E(\boldsymbol{V})/\theta_E(0)$ as a function of radial and tangential lens velocities V_z and $V_\perp$ (V_z positive for motion toward observer). Plotted contour values from 0.5 (*bottom right*) to 2 spaced by 0.1: dashed curves indicate values <1, the thick solid curve represents 1, and solid curves indicate values >1. The dot-dashed curve represents $V = 1$.

a finite result for the angular lens separation, and the scaled lens separation thus vanishes, $d(\boldsymbol{V}) \rightarrow 0$. Hence, such a binary lens would in effect behave like a single lens.

We note that in this regime the approximation of first order in deflection used in this paper eventually breaks down. However, the divergence of the Einstein radius is very slow, on the order of $\sim(1 - V)^{-1/4}$. From Figure 2 we can see that even for $V = 0.9$ the Einstein radius is at most greater by a factor of 2 (if the lens moves directly away). Even with a factor of 100 or more the approximation remains valid. It is thus sufficient to formally ignore the results for $V = 1$. This conclusion is in agreement with the results of Wucknitz & Sperhake (2004) for a lens moving radially away from the observer.

A lens moving with a velocity $V \rightarrow 1$ directly toward the observer would have a vanishing angular Einstein radius, $\theta_E(\boldsymbol{V}) \rightarrow 0$. The angular lens separation $\boldsymbol{\theta}_{AB} \rightarrow \boldsymbol{R}_\perp/D_L$, and the lenses appear to be at their "true" positions. The scaled lens separation thus diverges, $d(\boldsymbol{V}) \rightarrow \infty$. The decreasing Einstein radius means that such a binary lens would behave like two single lenses with decreasing strength as the lens moves together with the arriving photons.

4. DISCUSSION

In § 3.1 we have demonstrated the low-velocity effects for different binary lens orientations and intrinsic separations. Nevertheless, from the observational perspective we must take into account the fact that not all binary lens configurations necessarily lead to microlensing events detectable as two–point-mass lens events. Although this depends on the exact source trajectory, from a statistical point of view the Einstein radius–scaled projected lens separation d plays the main role. If the separation is too small or too large, most events would appear as single-lens events.

For an event to be detectable as a two–point-mass lens event, the lens separation has to fulfil $d(0) \in (d_{\min}, d_{\max})$, which leads to limits on the binary lens axis orientation:

$$\cos\zeta \in (d_{\min}, d_{\max}) \left(\frac{R}{4\ \mathrm{AU}}\right)^{-1} \frac{D_L}{4\ \mathrm{kpc}} \frac{\theta_E(0)}{1\ \mathrm{mas}}. \qquad (23)$$

The values of binary separations from the 21 binary events published by the MACHO team (Alcock et al. 2000) range from 0.421 to 2.077 with an outlier value of 7.454 (a possible binary source event). The 18 events detected by OGLE-II (Jaroszyński 2002) have values ranging from 0.355 to 2.917, and the values for the 15 events detected by OGLE-III (Jaroszyński et al. 2004) range from 0.352 to 3.457.

To obtain a rough empirical estimate we set $d_{\min} = 0.3$ and $d_{\max} = 4$. If we keep D_L and θ_E fixed at the values used in equation (23), for an intrinsic binary separation $R = 15$ AU we get limits on the axis angle $\zeta \in (0^\circ, 85^\circ)$, for $R = 60$ AU we get $\zeta \in (75^\circ, 89^\circ)$, and for $R = 240$ AU we get $\zeta \in (86^\circ, 89^\circ.7)$. In the first case we have a wide range of possible orientations; however, if we approach 90°, at which the velocity effects are strongest, it would be difficult to detect such an event as a binary lens event. The two cases with higher intrinsic separations demonstrate that such lenses can have stronger velocity effects while being detectable as binary events, albeit for a narrower range of axis orientations.

In this work we concentrated on the center-of-mass velocity of the binary lens and neglected its orbital velocity. However, for binaries or star+planet systems with semimajor axis $\ll 1$ AU the assumption of small orbital velocity breaks down. The results of this paper indicate that the velocity effects are proportional to the intrinsic lens separation, being caused by the lens motion during the passage of the light ray in its vicinity. Even though the orbital velocity grows as $R^{-1/2}$ with decreasing R, its product with the separation decreases as $R^{1/2}$. We conclude that the effects of *orbital* lens velocity on light deflection are not significant even in nonrelativistic binary lens systems closer than 1 AU.

5. SUMMARY

When we take into account general lens and source velocities, we find in the weak-field regime that single and two–point-mass gravitational microlensing obeys exactly the same lens equations as in the usual quasistatic approach. However, the parameters of the lens equation, such as the Einstein radius and the apparent binary lens separation, are velocity dependent, as shown in equations (14) and (13). These additional degeneracies have to be taken into account when we interpret the lens equation parameters and convert them to the underlying physical parameters.

An interesting feature of the single-lens result is the absence of an aberration effect on the orientation of the deflection angle. The obtained general results for both lens types are independent of the source velocity. Although at highly relativistic velocities the Einstein radius can be strongly increased or decreased depending on the direction of the motion, in the "low-velocity" Galactic microlensing settings the lens velocity affects mainly the apparent binary lens separation. The magnitude of the effect depends on the orientation of the binary axis and the lens velocity with respect to the plane of the sky; it can exceed 1% of the Einstein radius mainly for tangentially moving wide binary lenses aligned close to the line of sight.

We are grateful to the referee, Olaf Wucknitz, for his helpful comments and suggestions. This work was supported by grant GACR 205/04/P256 from the Czech Science Foundation.

REFERENCES

Alard, C., & Lupton, R. H. 1998, ApJ, 503, 325
Alcock, C., et al. 2000, ApJ, 541, 270
Boden, A. F., Shao, M., & Van Buren, D. 1998, ApJ, 502, 538
Brumberg, V. A. 1991, Essential Relativistic Celestial Mechanics (Bristol: Adam Hilger)
Frittelli, S. 2003, MNRAS, 340, 457

Han, C. 2001, MNRAS, 325, 1281
Jaroszyński, M. 2002, Acta Astron., 52, 39
Jaroszyński, M., et al. 2004, Acta Astron., 54, 103
Klioner, S. A. 2003, A&A, 404, 783
Kopeikin, S. M., & Schäfer, G. 1999, Phys. Rev. D, 60, 124002
Misner, C. W., Thorne, K. S., & Wheeler, J. A. 1973, Gravitation (New York: Freeman)
Paczyński, B. 1996, ARA&A, 34, 419
Pyne, T., & Birkinshaw, M. 1993, ApJ, 415, 459
Will, C. M. 1981, Theory and Experiment in Gravitational Physics (Cambridge: Cambridge Univ. Press)
Wucknitz, O., & Sperhake, U. 2004, Phys. Rev. D, 69, 63001